The Behaviour and Influence of Desiccation Cracking on a Full-Scale, Vegetated Infrastructure Embankment

R.A. Stirling, S. Glendinning, C.T. Davie
School of Engineering, Newcastle University, UK

R.M. Hen-Jones
Faculty of Engineering, University of Bristol, UK

P.N. Hughes
Department of Engineering, Durham University, UK

ABSTRACT: The mechanism behind desiccation cracking and its implications on earth structure stability have been under increasing study in recent decades, largely due to the uncertainty around our changing climate. The resilience of our geotechnical infrastructure to projected climate change is of particular concern, making the need to understand the complex soil-vegetation-atmosphere interaction all the more crucial. A diverse suite of instrumentation and geophysical techniques have been employed to gain a detailed understanding of embankment behaviour within the vadose zone subject to cycles of seasonal weather. Alongside soil-water content and matric suction sensing, high resolution linear displacement transducers have been used to track the highly sensitive crack aperture response to seasonal evapotranspiration trends and rainfall events. The transient influence of cracks on infiltration-runoff partitioning of rainfall has been investigated via runoff catchment monitoring. In addition to studying natural responses at the slope scale, 2D Electrical Resistivity Tomography has enabled visualisation of elevated water content 'plumes' beneath crack features. This paper highlights salient aspects of crack maturation, atmospheric field condition sensitivity, and the influence of vegetation presence on cracking and provides a reference point for full-scale, in situ behaviour of desiccation cracking beyond the constraints of laboratory settings.

1 INTRODUCTION

Desiccation cracking is observed in numerous contexts, from geotechnical engineering, mining and resource management to agriculture and process-materials engineering. Understanding the behaviour of compacted clay fills prone to environmentally driven cracking is of particular importance for infrastructure earthworks where structures are spatially extensive and expectations on long-term performance are high.

Compacted clay fills are subject to shrink-swell driven by transient soil-water content. This is primarily the result of seasonal fluctuation in precipitation/evaporation in addition to the effects of vegetation demand and the infiltration potential of the soil surface and is therefore largely governed by climate. Predicted UK climate change scenarios are recognised to have the capacity to more frequently bring about conditions conducive to increased desiccation cracking because of the increased occurrence of warmer and drier summers experiencing rainfall events of shorter duration and higher intensity (Hulme et al., 2002; Jenkins et al., 2010). Slope pore-water pressure response to rainfall events is heavily influenced by the enhanced infiltration capacity of cracked soils (e.g. Anderson et al, 1982, Rouainia et al. 2009).

Study of the desiccation cracking mechanism is typically conducted using laboratory experimentation (e.g. Nahlawi and Kodikara 2006, Peron et al, 2009, Tang et al, 2011) or by numerical simulation (e.g. Stirling et al, 2017, Vo et al. 2017). The size effect in soil cracking is well established (i.e. Lakshmikantha et al, 2012, Tollenaar et al. 2017) and yet, full-scale site-based studies are limited in number (e.g. Zhan et al. 2006; Dyer et al. 2009) with reports from densely vegetated slope sites representative of UK rail and highway networks particularly lacking from the literature. Understanding cracking in this situation is considered a fundamental step in the application of new and existing numerical tools to better assess the influence of cracking and climate on infrastructure slope stability.

2 RESEARCH EMBANKMENT

The BIONICS full-scale research embankment is a 6 m high, 90 m long embankment orientated in an east-west direction with a 1 in 2 slope that is representative of typical UK infrastructure (Figure 1). The embankment is located at Nafferton Farm, Stocksfield,

Northumberland, UK (Ordinance Survey grid Reference NZ 064 657).

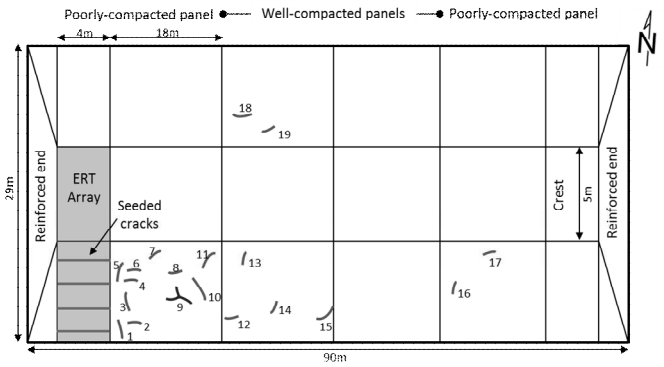

Figure 1. Embankment schematic depicting desiccation crack distribution.

2.1 *Construction and material*

The embankment was constructed in four 18 m long sections with the central sections constructed according to UK Highways Agency specifications (termed 'well compacted') and the two outermost sections built with reduced compaction to represent poorly constructed/heterogeneous rail embankments.
Further details of design, construction process, instrumentation and materials testing are provided in Hughes et al. (2009); its behaviour over a 4 year period is further discussed by Glendinning et al, (2014).

Embankment fill material was locally sourced glacial till (Durham Lower Boulder Clay). The Atterberg limits, tested in accordance with BS 1377 (1990), were 43% and 21% for Liquid and Plastic Limits respectively which classifies the material as intermediate plasticity. Compaction characterisation was conducted to BS 1377 (1990) using normal Proctor (light) compaction which found the maximum dry density to be 1.71 Mg/m^3 at a 15% optimum water content. Particle size distribution testing found the soil to be relatively well-graded in the portion >2 μm. The results of quantitative XRD analyses on the sub 2 μm fraction of the embankment fill material suggests that the clay mineral assemblages are generally similar and composed of variable amounts of illite/smectite (ranging from 42 to 54%, with a mean of 49%), chlorite/smectite (3–7% range, mean 5%), illite (16–26 % range, mean 19%) and kaolinite (23–31% range, mean 26%). Finally, the SWRC as determined by dewpoint potentiameter is presented in Figure 2.

2.2 *Embankment vegetation*

The slopes were seeded immediately after placement of 300 mm topsoil with a grassland/highways mixture typical of the North East of England. Vegetation surveys conducted in the period 2014-2015 indicate a shift towards wind-blown colonization by other plant species on the south facing slope. There exists

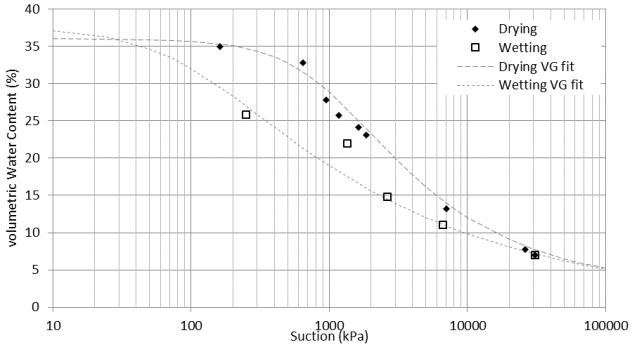

Figure 2. Soil-water retention curve (after Hen-Jones et al. 2017).

a marked difference between the north and south aspect, particularly evident in May-August time. The northern aspect is characterised by lower plant diversity, predominantly grasses (e.g. *Alopecurus pratense* (Meadow foxtail) and *Lolium perenne* (Perennial Ryegrass)) while the southern aspect accommodates a higher diversity of wildflowers (e.g. *Leucanthemum vulgare* (Oxeye Daisy), *Filipendula ulmaria* (Meadowsweet), *Achillea millefolium* (Yarrow) and *Knautia arvensis* (Field scabious))). Excavations conducted in the course of instrument installation indicated an average rooting depth of approx. 400 mm, below which rooting density diminishes.

2.3 *Embankment instrumentation*

Instrumentation comprises a catalogue of predominantly volumetric water content and soil-water potential sensors in addition to dual aspect meteorological monitoring and runoff catchments. The soil sensors employed were manufactured by Decagon Devices, namely the 5TE and MPS-1/2 and MPS-6 models. The 5TE measures the dielectric permittivity of the soil to determine the volumetric water content while the MPS range measures permittivity across a ceramic disc in equilibrium with soil-water to determine the water potential. In the interests of brevity, technical specifications for these sensors may be accessed directly from the manufacture's literature.

These sensors are typically located at the slope toe, mid-point and shoulder on both aspects on the western 'poorly' and well compacted panels. Installations were conducted at 0.5, 1.0 and 1.5 m depths within a spacing of no more than 150 mm at each monitored location.

3 CRACK SURVEYING

A campaign of manual crack surveys was carried out annually from 2009-2015 and typically during the months of June-August. Crack observations comprised their location, length, width at regular intervals along the length and approximate depth – established manually by gradated probe (discussed further by Eminue et al. at this conference). This process is

inherently labour intensive and relies upon successful discovery of crack sites amongst what is usually tall vegetation in this period (up to 0.5 m). This factor is particularly important in the discovery of newly initiated cracks since once established, crack sites can often be reliably studied year on year.

Figure 3 shows a crack seen on the embankment (Crack 4 – Figure 1). Linear cracks with limited branching are almost exclusively seen in this context and indicate the significant influence of vegetation presence, likely a result of root mass reinforcement.

Desiccation cracking research, both physical and numerical commonly focuses upon crack reproduction in a laboratory setting using processed clays. Therefore, the scale is rarely representative of field conditions and such experiments struggle to account for heterogeneity as observed in full-scale structure materials – a fundamental consideration in stress localisation. This makes the understanding of cracking in the field, over long time scales particularly important if existing research into cracking is to be applicable to geotechnical infrastructure.

Figure 3. Typical linear cracking style on vegetated slope infrastructure in UK.

4 HIGH RESOLUTION MONITORING

To understand the behaviour of desiccation cracks at full-scale on vegetated infrastructure slopes, linear transducers were installed across an active crack site (Figure 4). The site selected was crack 9 shown in Figure 1. This crack is positioned towards the centre of the south facing 'poorly' compacted panel and as such is considered to not be influenced by any boundary effect as a result of embankment construction. Crack surveying identified this crack as being representative of typical crack activity.

Figure 4. Transducer configuration at monitored crack site.

4.1 *Crack monitoring installation*

The three stainless steel transducers had a 200 mm stroke range and were capable of operating between -40 to +150°C using contactless (inductive coil) sensing. At the time of installation, grass cover was cut back to expose the crack, as depicted in Figure 4 by the white line. PVC plates fitted with six 80 mm spikes were used to fix each transducer end to opposing sides of the crack. Care was taken not to place the fixings too close to the crack aperture so not to disturb the crack as well as to leave sufficient travel to accommodate either direction of movement following installation.

4.2 *Crack response to environmental conditions*

The behaviour of the crack from May 2015 to November 2016 is presented in terms of transducer displacement in Figure 5. Also presented is corresponding volumetric water content and soil matric suction data from a monitoring profile 1.6 m away from the crack site. Rainfall, potential evapotranspiration (ETo) and runoff data is also presented for the same period. A diurnal signal in transducer displacement was detected with a maximum of 1.5 mm recorded.

The crack transducers indicate the onset of crack aperture opening at the start of June. This aligns well with the onset of suction generation as measured at 0.5 m depth and follows a period of limited rainfall and high ETo. Once open, a series of rainfall events are shown to produce a response in suction and most noticeably, result in a rapid reduction in crack aperture (highlighted). Continued high levels of ETo during this period is seen to maintain suctions between 200-320kPa, enabling the crack to re-open between the three major rainfall events.

Transducer 1 exhibits the greatest response to environmental variation. However, all three transducers capture the interaction between dominant ETo and punctuated rainfall events throughout the summer months. Following the fourth highlighted rainfall event, total ETo reduces and rainfall dominates. The crack aperture is shown to reduce consistently from October to mid-November 2015, with assumed closure (return to original displacement in transducers 1 and 2) simultaneously with the loss in suctions.

During the 2015-2016 winter, little to no displacement is evident on the monitored crack. Relatively high water content is sustained suggesting saturated conditions which result in previously undetectable runoff following high rainfall (January 2016).

Transducers were disturbed in mid-March through April 2016. This is attributed to burrowing activity observed across the embankment by rabbits (*Oryctolagus cuniculus*). The influence of macrobiota on the enhancement of infiltration on vegetated slopes is a little addressed aspect of ecological-geotechnical engineering.

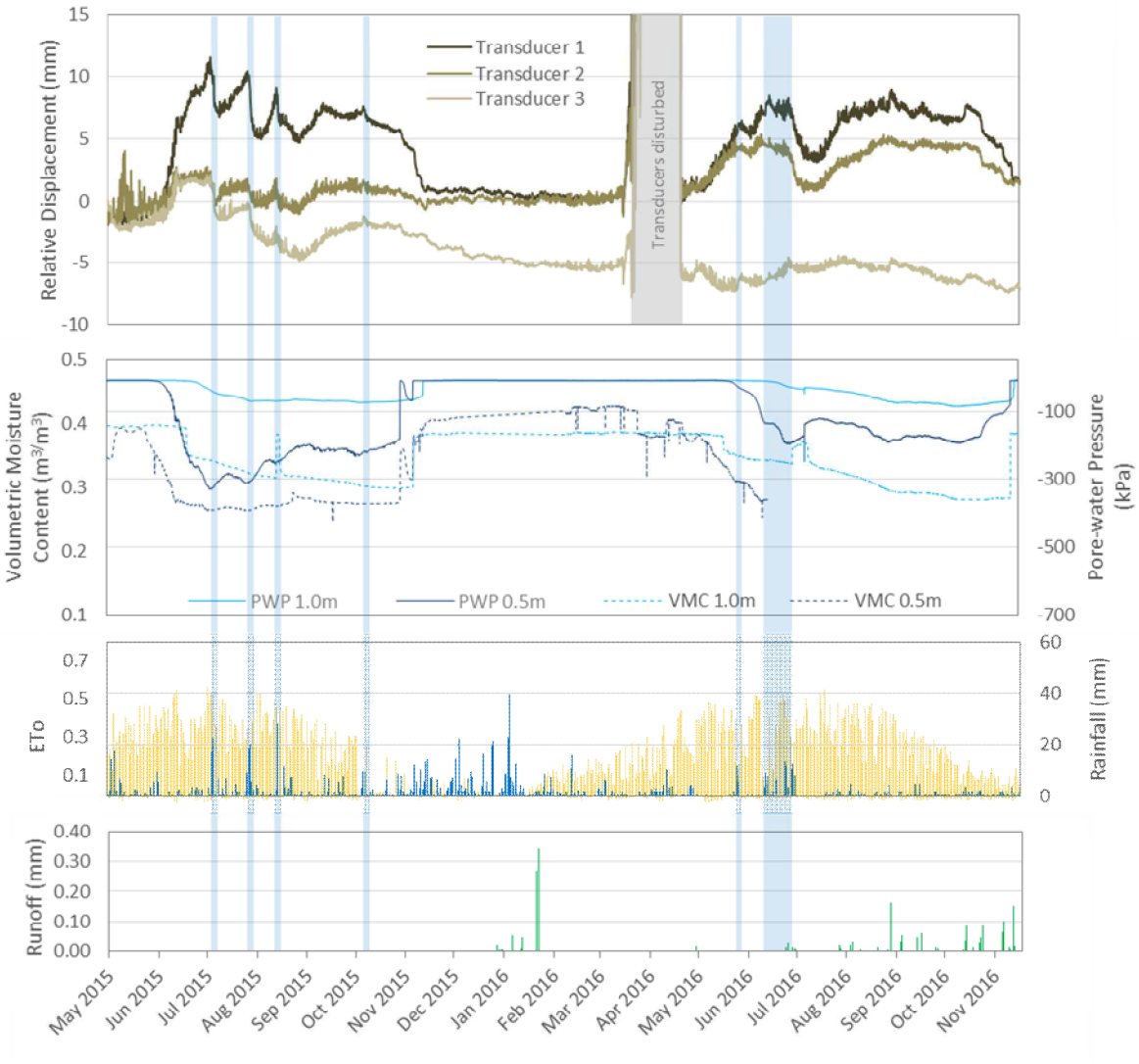

Figure 5. Crack and environmental monitoring time series data.

Despite its obvious difference in mechanism, it is recognised to have a not insignificant deteriorative effect on a wide range of geotechnical infrastructure.

In 2016, the crack aperture is again shown to open in May during a period of sustained high ETo and low rainfall. The rapid response of crack displacement to rainfall events is seen again, although unlike the previous year, a wet period late-June – July is experienced which limited the development of deeper suctions and results in measurable runoff.

There exists a clear connectivity between cracking behaviour, near-surface (<1 m) saturation and runoff. Taking the period May-May, despite relatively high rainfall events during the active crack season, no runoff is measured.

Conversely, once the crack is assumed to have closed (post- mid-November 2015), runoff is produced from similar magnitude rainfall events. Although the occurrence of runoff is linked to soil surface saturation, it is also considered that reduced runoff is linked to the presence of open cracks on the slope surface and that these result in the interception of this flow. Therefore, the infiltration potential of cracking is necessary to progress the understanding of these transient and dynamic features.

5 CRACK DEVELOPMENT USING ERT

A 4m wide x 6m high, south-facing slope section to the west of the embankment (Figure 1) is the site of a 3D electrical resistivity tomography (ERT) array operated by the British Geological Survey and Newcastle University. The array comprises a total of 281 electrodes at 0.7m grid spacing, arranged with a dipole-dipole configuration, which is highly-sensitive to horizontal resistivity variations. Alternating pairs of electrodes are used to impart current and to record the resulting change in potential. This is then related to resistance via Ohm's law (V=IR), and corrected for geometry, allowing the volumetric subsurface resistivity distribution to be imaged. Due to the sensitivity of resistivity to temperature, standard procedure is to correct images to a reference value, which in this study was taken to be the mean annual air temperature at the embankment site, 9.35°C. The basic principal of the ERT method as a tool for imaging moisture dynamics is that low water content corresponds to high resistivity values, and vice versa.

The ERT array took measurements on an approximately daily basis. The images presented here show "slices", extracted along the central line of the array from 3D volumetric images during a period of rapid drying over the course of summer 2013. Figure 6a shows the initial resistivity distribution recorded on 15th June, and highlights the highly permeable crest ballast (approx. 150-250 Ωm), the near-saturated embankment core (approx. 20-50 Ωm) and a stratified slope flank. The following images present the ratio change in resistivity with respect to the first date - the associated colour scale has been chosen to highlight features characterised by a resistivity increase greater than 30 % (orange to red).

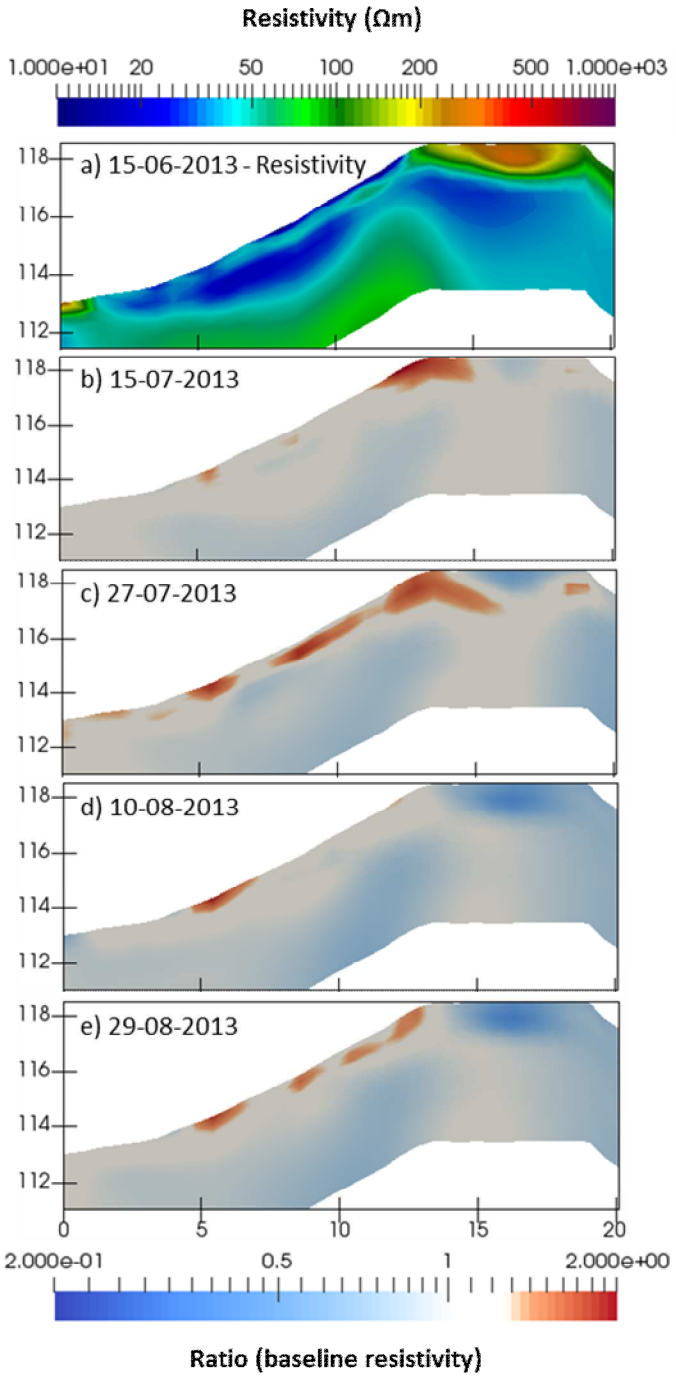

Figure 6. Developing crack features as imaged using electrical resistivity.

The development of crack features on the Southern flank of the BIONICS embankment may be imaged, which tallies with observations made during field surveys over the same period. The development of these crack features may be described as follows: in Figure 6b (15th July 2013), taken one month after the initial resistivity distribution image, significant drying has occurred at the south-facing portion of the crest ballast, extending into the fill material, this is attributed to the embankment orientation. The south-facing aspect of the ERT monitored section is exposed to both the prevailing wind direction (South-westerly) and the longest daily sunshine making this region experience the greatest degree of evapotranspiration. The influence of slope exposure is further demonstrated by the prevalence of cracking to the south-west end of the embankment (Figure 1).

Further down the slope flank, localised increases in resistivity are observed at 5.5 and 8m, corresponding to the locations of known cracks from previous field surveys; walkover surveys confirmed the presence of these cracks during the summer 2013 period.

By 27th July (Figure 6c), the two crack features have increased in volume, and much of the upper 1m of the slope flank is characterised by significant resistivity increases; observations during this time described significant extensive drying of the topsoil. Following heavy rainfall over the subsequent two weeks, the embankment surface wets up rapidly, and on 10th August (Figure 6d), only the bottom anomaly is visible, as the other features heal due to swelling associated with infiltration of rainwater into the clay fill. Drying of the near-surface then resumes: on 29th August, (Figure 6e), the anomalies have increased in volume, clearly illustrating four distinct crack locations where soil resistivity has increased by more than 30 % with respect to the baseline date at the start of the summer drying period. As well as being noted during summer 2013 field surveys, these four cracks are reoccurring features captured in multiple annual field surveys. In Figure 7, the resistivity distribution for the same embankment segment is shown during the winter of the following year (December 2014; scale same as in Figure 6).

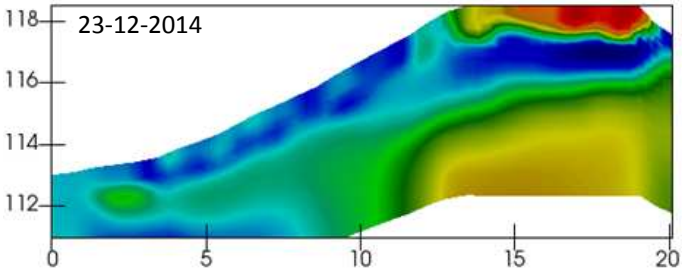

Figure 7. Low resistivity values associated with elevated water contents beneath crack locations.

Blue contours highlight low resistivity values in the vicinity of the existing crack locations. These values are associated with elevated water content "plumes"

arising from infiltration of rainwater via the cracks, and demonstrate the capacity of ERT imaging to capture the soil response to both rapid drying and wetting, in terms of crack development and evolution.

6 CONCLUSIONS

An overview of desiccation cracking in a full-scale, vegetated UK infrastructure-style embankment is presented, which for the first time, includes quantitatively the transient behaviour of cracking in the field.

Characterisation of cracking in densely grassed slopes is established and the contrast in style between these observed features and those commonly reproduced in the laboratory is highlighted. The influence of compaction (e.g. Victorian vs. modern highway specification) and slope aspect (i.e. exposure to prevailing wind direction) is demonstrated to have a significant effect on the distribution and extent of cracking.

The sensitivity of crack aperture to underlying unsaturated soil conditions and the atmospheric conditions that drive them in the near-surface is shown. The seasonal life-cycle of these features is also presented in parallel with rainfall-runoff monitored data which has enabled the implications of crack-based infiltration to be considered.

Lastly, the ability of ERT to provide visualisation capability to identify isolated crack features is presented. The development of these features during the summer of 2013 is depicted in addition to the ultimate implication of crack presence – namely, enhanced infiltration capacity.

7 ACKNOWLEDGEMENTS

The authors would like to acknowledge the collaborative research projects iSMART (Grant number EP/K027050/1) and ATU (Grant number EP/K021699/1) funded by the UK Engineering and Physical Sciences Research Council (EPSRC).

8 REFERENCES

Anderson, M.G., Hubbard, M.G. & Kneale, P.E. 1982. The Influence of Shrinkage Cracks on Pore-Water Pressures Within a Clay Embankment. *Quarterly Journal of Engineering Geology and Hydrogeology* 15: 9-14.

British Standards 1990. Methods of test for Soils for civil engineering purposes 1377- Part 2: Classification tests. London: British Standards Institution.

British Standards 1990. Methods of test for Soils for civil engineering purposes 1377- Part 4: Compaction related tests. London: British Standards Institution.

Dyer, M., Utili, S. & Zielinski, M. 2009. Field survey of desiccation fissuring of flood embankments. *Water Management* 162(WM3): 221-232.

Glendinning S., Hughes P.N., Helm P., Chambers J., Mendes J., Gunn D., Wilkinson P. & Uhlemann S. 2014. Construction, management and maintenance of embankments used for road and rail infrastructure: implications of weather induced pore water pressures. Acta Geotechnica 9: 799–816.

Hen-Jones, R.M., Hughes, P.N., Stirling, R.A., Glendinning, S., Chambers, J.E., Gunn, D.A. & Cui, Y.J. 2017. Seasonal effects on geophysical–geotechnical relationships and their implications for electrical resistivity tomography monitoring of slopes. *Acta Geotech* 12(5): 1159-1173.

Hughes P.N., Glendinning S., Mendes S., Parkin G., Toll D.G., Gallipoli D. & Miller P.E. 2009. Full scale testing to assess climate effects on embankments. *Engineering Sustainability* 162(2): 67-79.

Hulme, M. Jenkins, G.J., Lu, X., Turnpenny, J.R., Mitchell, T.D., Jones, R.G., Lowe, J., Murphy, J.M., Hassell, D., Boorman, P., McDonald, R. & Hill, S. 2002. Climate Change Scenarios for the United Kingdom. The UKCIP02 Scientific Report, Tyndall Centre, School of Environmental Sciences, UK.

Jenkins, G., Murphy, J., Sexton, D., Lowe, J., Jones, P. & Kilsby, C. 2010. UK Climate Predictions Briefing Report, UK Climate Impacts Programme.

Lakshmikantha, M.R., Prat, P.C. & Ledesma, A. 2012. Experimental evidence of size effect in soil cracking. *Canadian Geotechnical Journal* 49(3): 264-284.

Nahlawi, H. & Kodikara, J.K. 2006. Laboratory experiments on desiccation cracking of thin soil layers. *Geotechnical and Geological Engineering* 24: 1641-1664.

Peron, H., Hueckel, L., Laloui, L. & Hu, L.B. 2009. Fundamentals of desiccation cracking of fine-grained soils: experimental characterisation and mechanisms identification. *Canadian Geotechnical Journal* 46(10): 1177-1201.

Rouainia, M., Davies, O., O'Brien, T. & Glendinning, S., 2009. Numerical Modelling of Climate Effects on Slope Stability. *Engineering Sustainability* 162(ES2): 81-89.

Stirling, R.A., Glendinning, S. & Davie, C.T. 2017. Modelling the deterioration of the near surface caused by drying induced cracking. *Applied Clay Science* 146: 176–185.

Tang, C.-S., Shi, B., Liu, C., Suo, W.-B. & Gao, L. 2011. Experimental characterization of shrinkage and desiccation cracking in thin clay layer. *Applied Clay Science* 52(1–2): 69-77.

Tollenaar, R.N., van Paassen, L.A. & Jommi, C. 2017. Observations on the desiccation and cracking of clay layers. *Engineering Geology* 230: 23-31.

Vo, T.D., Pouya, A., Hemmati, S. & Tang, A.M. 2017. Numerical modelling of desiccation cracking of clayey soil using a cohesive fracture method. *Computers and Geotechnics* 85: 15-27.

Zhan, T., Ng, C. & Fredlund, D.G. 2006. Instrumentation of an Unsaturated Expansive Soil Slope. *Geotechnical Testing Journal* 30(2): 1-11.